

Thermodynamic Stability of Metastable Tetragonal t' - $\text{Ce}_{0.5}\text{Zr}_{0.5}\text{O}_2$ Phase in the CeO_2 - ZrO_2 system

Shinya Otsuka-Yao-Matsuo*, Takayuki Yao, and Takahisa Omata

*Department of Materials Science and Processing, Graduate School of Engineering,
Osaka University, Yamada-oka 2-1, Suita 565-0871, Japan*

(Received: May 6, 2003)

SYNOPSIS

According to the XRD analysis and emf measurements employing a solid electrochemical cell, we have compared the thermodynamic stabilities of metastable t' - $\text{Ce}_{0.5}\text{Zr}_{0.5}\text{O}_2$ phase, ZrO_2 -based monoclinic and CeO_2 -based cubic phases (m+c) mixture, and ZrO_2 -based tetragonal and CeO_2 -based cubic phases (t+c) mixture. The present experiments have confirmed that the t' phase is metastable at higher temperatures than 1373 K, and the stable state is (t+c) mixture. The t' phase is metastable at lower temperatures than 1173 K, and the stable state is (m+c) mixture. These results are consistent with the equilibrium phase diagram of CeO_2 - ZrO_2 system. According to the emf measurements, it was found that the thermodynamic stability of the t' phase lies between those of (t+c) and (m+c) at lower temperatures than 1173 K. It was concluded that the t' phase is metastable, but its thermodynamic stability is close to those of (t+c) and (m+c).

Keywords: metastable phase, thermodynamic stability, phase diagram, ceria, zirconia

1. INTRODUCTION

CeO_2 - ZrO_2 powders are promising materials as sub-catalysts for automotive exhaust gases /1-4/, because harmful CO and hydrocarbon gases in exhaust gases can be oxidized to harmless CO_2 and H_2O gases by the oxygen released from the powders. The CeO_2 - ZrO_2 based oxides may be also useful as the electrode for solid oxide fuel cell (SOFC) /5,6/, because they exhibit high mixed-conduction of oxygen ion and electron. In the intermediate composition range of the equilibrium phase diagram reported in the CeO_2 - ZrO_2 system, no compound exists except for cubic CaF_2 -type $(\text{Ce}_x\text{Zr}_{1-x})\text{O}_2$ phases over 1823 K /7,8/. At intermediate temperatures, monoclinic ZrO_2 -based and cubic CeO_2 -based phases below 1323 K and tetragonal ZrO_2 -based and cubic CeO_2 -based phases above 1323 K coexist, respectively. In the range of $x=0.2\sim0.7$, when the cubic CaF_2 -type $(\text{Ce}_x\text{Zr}_{1-x})\text{O}_2$ phase is cooled in the furnace, in spite of its low cooling rate, a tetragonal t' form maintaining random distribution of Ce and Zr ions can appear through a cation diffusionless phase transition without the phase separation /8-10/. It has been believed that the t' form is a metastable phase. There is another

* Corresponding authors: Shinya Otsuka-Yao-Matsuo

Department of Materials Science and Processing, Graduate School of Engineering,
Osaka University, 2-1 Yamada-oka, Suita 565-0871, Japan
Tel.+81-6-6879-7461, Fax. +81-6-6879-7461
e-mail: shinya@mat.eng.osaka-u.ac.jp

metastable phase established recently, i.e., κ - CeZrO_4 and t'_{meta} phases [11,12]. When the pyrochlore-type $\text{Ce}_2\text{Zr}_2\text{O}_{7+y}$ obtained by the reduction of the t' phase was oxidized at a low temperature, e.g., 873 K, oxygen was intercalated maintaining the ordered arrangement of Ce and Zr ions in the resulting phase and then the metastable κ - CeZrO_4 phase appears [4,11,13].

It has been reported that the metastable κ - CeZrO_4 phase transformed to the t' - $\text{Ce}_{0.5}\text{Zr}_{0.5}\text{O}_2$ phase above 1323 K [14]. At temperatures as high as 1423 K, the t' phase did not decompose into the tetragonal ZrO_2 -based and cubic CeO_2 -based phases [14,15]. The t' phase is thermally fairly stable, although it is possibly a metastable phase. The objective of the present study is to confirm the thermodynamic instability of the t' - $\text{Ce}_{0.5}\text{Zr}_{0.5}\text{O}_2$ phase, in comparison with those of the mixed phases of the monoclinic ZrO_2 -based (m-phase) and cubic CeO_2 -based (c-phase) phases and the mixed phases of the tetragonal ZrO_2 -based (t-phase) and cubic CeO_2 -based (c-phase) phases.

2. EXPERIMENTAL

Experimental principle

In the present investigation, the electrochemical cell I: Pt, $\{t', (m+c), \text{ or } (t+c)\} + \text{Ce}_2\text{Zr}_2\text{O}_{7+y} / \text{ZrO}_2(+\text{Y}_2\text{O}_3) / \text{air}$, Pt, involving a solid electrolyte, was constructed for the determination of the equilibrium partial pressure of O_2 over the mixtures along the $x_{\text{Ce}}/x_{\text{Zr}}=1$ of the total composition which can be noted as $\text{Ce}_2\text{Zr}_2\text{O}_{8-z}$ [16]. The value of z ranges from 0 to 1. $z=0$ corresponds to a single or two phases of the CeO_2 - ZrO_2 system, while $z=1$ corresponds to the pyrochlore $\text{Ce}_2\text{Zr}_2\text{O}_7$ phase alone. The emf, E of the cell I is related to the partial pressure of O_2 , $p(\text{O}_2)$, over the mixtures, according to [17]

$$E = (RT/4F) \ln \{p(\text{O}_2)/0.21 p^*\} \quad [1]$$

where R is the gas constant ($8.31441 \text{ J mol}^{-1} \text{ K}^{-1}$), T is the experimental temperature (K), F is Faraday's constant ($96484.56 \text{ C K}^{-1}$), and $p^*=101325 \text{ Pa}$.

In the Ce-Zr-O ternary system, the Gibbs-Duhem equation can be written as

$$x_{\text{Ce}}\mu_{\text{Ce}} + x_{\text{Zr}}\mu_{\text{Zr}} + x_{\text{O}}\mu_{\text{O}} = 0 \quad [2]$$

where μ_i is the chemical potential of the component, i.

Under the condition of $(x_{\text{Ce}}/x_{\text{Zr}})=1$, Eq. [2] becomes

$$d\mu_{\text{Ce}} + d\mu_{\text{Zr}} = -(x_{\text{O}}/x_{\text{Ce}})d\mu_{\text{O}} \quad [3]$$

If the variation of μ_{O} with composition along $(x_{\text{Ce}}/x_{\text{Zr}})=1$ is known, then we integrate Eq. [3] in the composition range of $z=0$ to $z=1$. After successive derivations [16,18], finally the standard Gibbs energy change for the reaction: $1/4\text{Ce}_2\text{Zr}_2\text{O}_7 + 1/8 \text{O}_2 \rightarrow \text{Ce}_{0.5}\text{Zr}_{0.5}\text{O}_2$ can be expressed as

$$\Delta G^\circ = (RT/8) \ln p(\text{O}_2) dz \quad [4]$$

The detailed derivation procedure was described elsewhere [16]. If the pyrochlore type $\text{Ce}_2\text{Zr}_2\text{O}_7$ could be equilibrated with t' - $\text{Ce}_{0.5}\text{Zr}_{0.5}\text{O}_2$, the value of $p(\text{O}_2)$ is constant, and therefore Eq.[4] becomes

$$\Delta G^\circ = (RT/8) \ln p(\text{O}_2) \quad [5]$$

One can understand that the equilibrium oxygen partial pressure, $p(\text{O}_2)$, decreases with increasing the thermodynamic stability of the $\text{Ce}_{0.5}\text{Zr}_{0.5}\text{O}_2$ phase. When $\text{Ce}_{2+y}\text{Zr}_{2-y}\text{O}_7$ is equilibrium with t' - $\text{Ce}_{1-x}\text{Zr}_x\text{O}_2$, i.e., the equilibrium tie-line does not lie on $(x_{\text{Ce}}/x_{\text{Zr}})=1$, the value of $p(\text{O}_2)$ over the mixture varies with the composition z , and therefore we have to use Eq. [4]. When the state for $(x_{\text{Ce}}/x_{\text{Zr}})=1$ in the CeO_2 - ZrO_2 system is a two phase-mixture, for instance, the mixture of c- CeO_2 based (c-phase) and m- ZrO_2 based (m-phase) phases, the oxygen partial pressure, $p(\text{O}_2)$, measured along the composition of $(x_{\text{Ce}}/x_{\text{Zr}})=1$ can be related to the thermodynamic stability of the mixture, the chemical potential of which is expressed by $\{(1-x_{\text{c-phase}})\mu_{\text{c-phase}} + x_{\text{m-phase}}\mu_{\text{m-phase}}\}$.

With increasing temperature, the mutual solubility of the tetragonal ZrO_2 -based (t-phase) and cubic CeO_2 -based (c-phase) phase became significantly dependent on the temperature. Therefore, instead of the emf measurement, we carried out the X-ray diffraction analysis of the tetragonal ZrO_2 -based (t-phase), cubic CeO_2 -based (c-phase), and t' - $\text{Ce}_{0.5}\text{Zr}_{0.5}\text{O}_2$ phases

mixture before and after annealed at preselected temperatures. The XRD patterns were compared and the thermodynamic instability of the t' - $\text{Ce}_{0.5}\text{Zr}_{0.5}\text{O}_2$ phase was discussed.

Sample preparation

The single phase of t' - $(\text{Ce}_{0.5}\text{Zr}_{0.5})\text{O}_2$ was first prepared by a conventional ceramic method. Powdered raw materials of cubic CeO_2 (Na, <100ppm; Fe, <10ppm) and monoclinic ZrO_2 (HfO_2 , <3.8 mass%, Na, <100ppm, Fe, <100ppm), which were supplied by Santoku Kinzoku Kogyo Co., Ltd, were thoroughly mixed at a molar ratio of 1:1 using a ball mill in a zirconia container, and pressed into 17.2 mm-diameter disks under 100 MPa. The pellets were sintered in air at 1923 K for 50 h to attain a single phase with a cubic CaF_2 -type structure. When the obtained disks were cooled by cutting the electric power off the furnace, the phase became single t' - $(\text{Ce}_{0.5}\text{Zr}_{0.5})\text{O}_2$. Some of the t' pellet was used without milling as a sample for a powder X-ray diffraction (XRD) analysis (Mac Science, MXP¹⁸, Cu- K_α radiation using a curved graphite receiving monochrometer). After the remaining t' pellets were crushed into grains, and then loaded in an alumina tube, which was quipped in a conventional electric furnace. On passing $\text{Ar}+1\%\text{H}_2$ gas at a flow rate of $100\text{ cm}^3\text{ min}^{-1}$, the sample was heated and kept at 1573 K for 10 h to obtain a pyrochlore-type $\text{Ce}_2\text{Zr}_2\text{O}_{7+y}$. The reduced sample was unloaded and weighed. The value of y for this sample was determined from the change in sample weight by the reduction. The value of y was 0.02 to 0.04; that is, the reduction ratio was 96 to 98 %. The obtained pyrochlore-type $\text{Ce}_2\text{Zr}_2\text{O}_{7+y}$ was used for the emf measurement. The powder was mixed with the CeO_2 powder at a 1:1 mol ratio and annealed at 1073 K for 20 h; the (m+c) mixed phases obtained were for the emf measurement. When the monoclinic ZrO_2 and cubic CeO_2 powders mixed at a 1:1 mol ratio were annealed at 1673 K for 50 h, the mixture became the (c+t) phases. The annealed mixture was used for the emf measurement. The details of experimental procedures on the emf measurements have been described previously /16/.

3. EXPERIMENTAL RESULTS AND DISCUSSION

XRD analysis

Fig. 1 shows the XRD patterns of the sample disks obtained by annealing t' - $(\text{Ce}_{0.5}\text{Zr}_{0.5})\text{O}_2$ pellets for 50 h in air at various temperatures. When the annealing temperature was 1473 K, the phase remained the t' - $(\text{Ce}_{0.5}\text{Zr}_{0.5})\text{O}_2$ as prepared. The diffraction peak indexed by 112 was observed, as shown in Fig.1 (c), which is the characteristic diffraction peak for the tetragonal t' form as well as for t form. When another t' disk was heated at 1488 K, small diffraction peaks due to the c and t phases

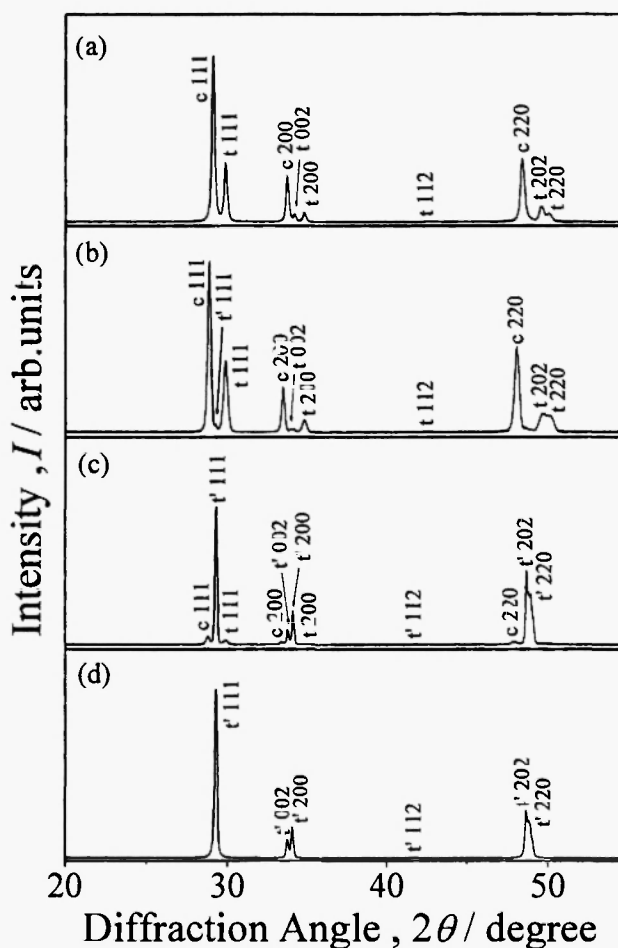


Fig. 1: XRD patterns of the samples obtained by annealing t' - $(\text{Ce}_{0.5}\text{Zr}_{0.5})\text{O}_2$ pellets at several temperatures.

(a) at 1673 K, (b) at 1573 K, (c) at 1488 K, (d) at 1473 K.

appeared. The diffraction peaks became higher with increasing the annealing temperature. Fig. 2 shows the XRD patterns of the sample disks obtained when the t' - $(\text{Ce}_{0.5}\text{Zr}_{0.5})\text{O}_2$ phase with the small amounts of precipitated $(t + c)$ phases was annealed at lower temperatures than 1488 K. The starting sample disk of $(t' + t + c)$ was prepared by annealing the t' - $(\text{Ce}_{0.5}\text{Zr}_{0.5})\text{O}_2$ disk at 1523 K for 20 h in air; the XRD patterns of the starting $(t' + t + c)$ sample prepared is shown in Fig. 2 (c). When the $(t' + t + c)$ disk was annealed at 1323 K for 50 h, no difference for the XRD patterns was observed. However, when the disk was annealed at 1373 K for 50 h, the diffraction peaks due to

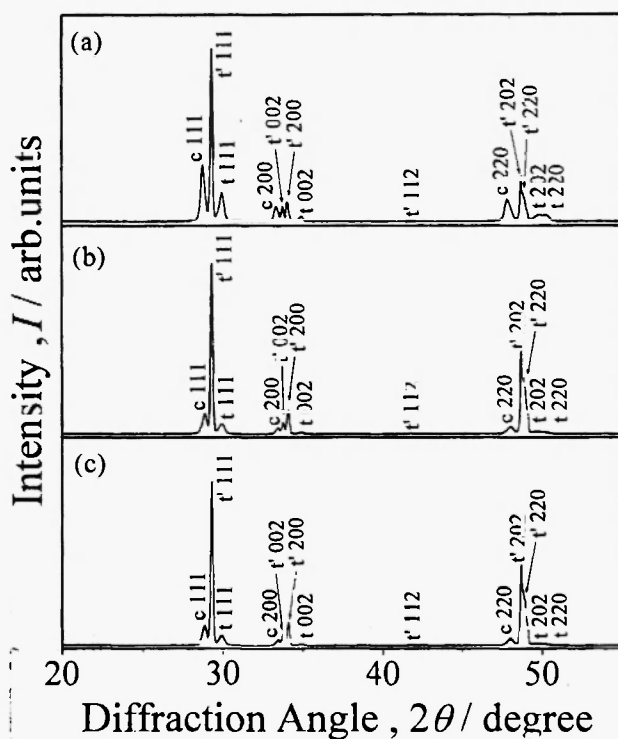


Fig. 2: Change in XRD patterns of the samples annealed obtained by annealing $(t'+t+c)$ mixed phases.

- (a) the sample obtained by annealing the sample(c) successively at 1373 K for 50 h,
- (b) the sample obtained by annealing the sample(c) successively at 1323 K for 50 h,
- (c) the starting sample obtained at annealing t' at 1523 K for 20 h.

c -phase and t -phase was increased; that is, the decomposition of t' -phase to c - and t -phases proceeded at 1373 K. The experimental results confirms that the $(t + c)$ two phases is thermodynamically stable at higher temperature than 1373 K at least, and the t' phase is metastable. The result is consistent with the equilibrium phase diagram of CeO_2 - ZrO_2 system. However, the t' phase is virtually stable at temperatures as high as 1473 K, because the precipitation of $(t + c)$ phases in the t' phase requires the nucleus.

Typical emf data for composition $\text{Ce}_2\text{Zr}_2\text{O}_{8-z}$ with $z=0.50$ are shown in Fig. 3. The small symbols indicate emf values observed at intervals of 5 min in the heating or cooling process; the heating and cooling rate was $3 \sim 5 \text{ K min}^{-1}$. The large symbols indicate stable emfs confirmed by keeping the sample at a preselected temperature on the way of the heating or cooling. The

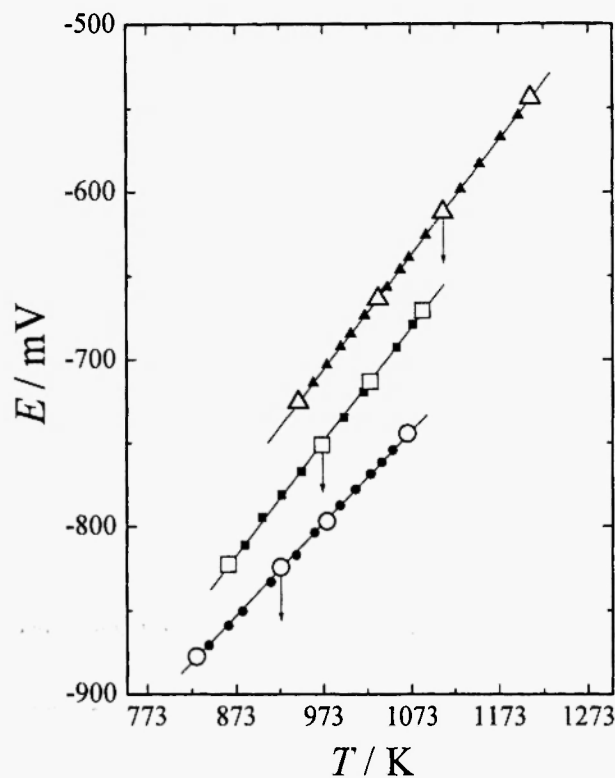


Fig. 3: The emf E of cell as a function of temperature, obtained when the mixtures with the total composition $z=0.5$ in $\text{Ce}_2\text{Zr}_2\text{O}_{8-z}$.

- \triangle —: $c+t$ +pyrochlore,
- \square —: t' +pyrochlore,
- \circ —: $m+t$ +pyrochlore.

least squares treatment of the stable emf values indicated by the large symbols gave the following equations.

For $z=0.50$,

$$E/\text{mV} = -1376.6 + 0.6887T \text{ for (c+t+pyrochlore)} \quad [6]$$

$$E/\text{mV} = -1413.9 + 0.6831T \text{ for (t'+pyrochlore)} \quad [7]$$

$$E/\text{mV} = -1333.1 + 0.5498T \text{ for (m+t+pyrochlore)}. \quad [8]$$

Typical emf data for composition $\text{Ce}_2\text{Zr}_2\text{O}_{8-z}$ with $z=0.20$ are shown in Fig. 4. The least squares treatment of the stable emf values indicated by the large symbols gave the following equations.

For $z=0.20$,

$$E/\text{mV} = -1423.6 + 0.7588T \text{ for (c+t+pyrochlore)} \quad [9]$$

$$E/\text{mV} = -1446.0 + 0.7601T \text{ for (t'+pyrochlore)} \quad [10]$$

$$E/\text{mV} = -1319.2 + 0.5373T \text{ for (m+t+pyrochlore)}. \quad [11]$$

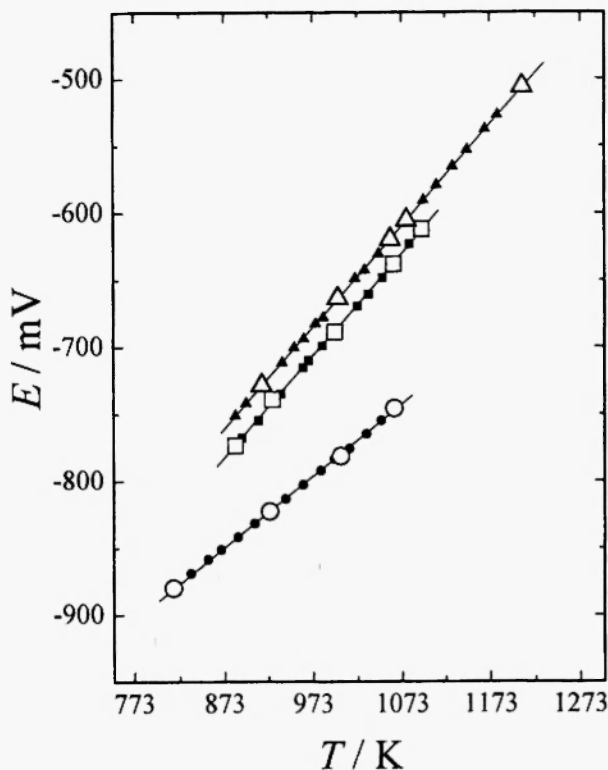


Fig. 4: The emf E of cell as a function of temperature, obtained when the mixtures with the total composition $z=0.2$ in $\text{Ce}_2\text{Zr}_2\text{O}_{8-z}$.

— \triangle \blacktriangle —: c+t+pyrochlore,

— \square \blacksquare —: t'+pyrochlore,

— \circ \bullet —: m+t+pyrochlore.

After the emf measurements were terminated, the stabilized-zirconia tube with sample powders at $z=0.50$, which were maintained at temperatures indicated by \downarrow in Fig. 3, were taken out of the furnace and cooled rapidly in air. Figs. 5, 6, and 7 show the XRD patterns of the sample powders before and after the emf measurements. As shown in Fig. 5, after the annealing of (t'+pyrochlore), the diffraction peaks due to pyrochlore shifted slightly toward higher angles. The split of the diffraction due to t', which is characteristic of tetragonal phase, became unclear. These indicate that the t' and pyrochlore phases have a slight mutual solubility. However, the XRD results confirm that the phases of the sample powders essentially consisted of the t' and pyrochlore phase after as well as before the emf measurement. As shown in Figs. 6 and 7, in the case of (c+t+pyrochlore) and (c+m+pyrochlore), the phases of the samples did not change essentially through the emf measurements much like (t'+pyrochlore).

As seen in Figs. 3 and 4, the emf values became negatively large in the order of (c+t+pyrochlore), (t'+pyrochlore) and (c+m+pyrochlore); that is, the

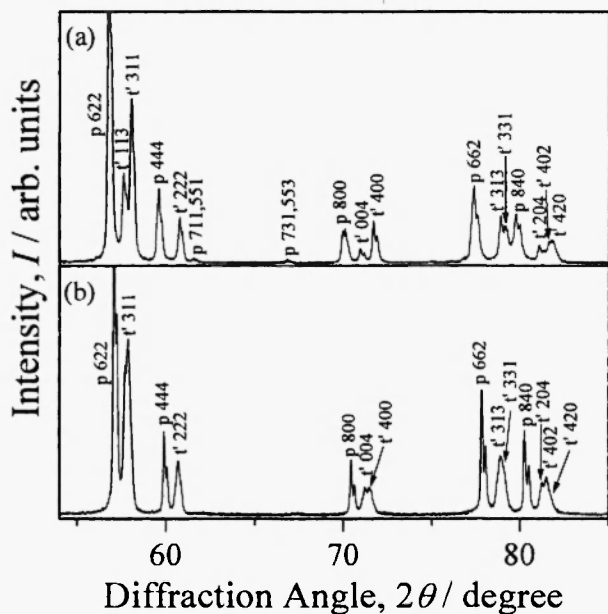


Fig. 5: XRD patterns of the samples when (t'+pyrochlore) mixtures with $z=0.5$ was used as the starting sample for the emf measurement.

(a): starting sample, (b): quenched at 973 K.

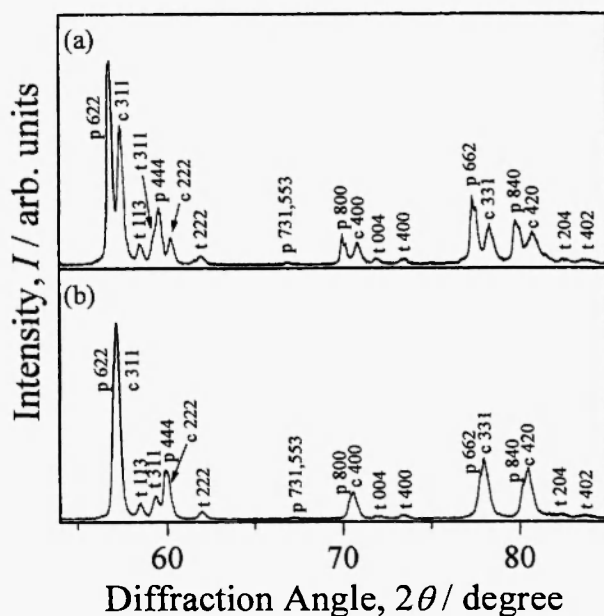


Fig. 6: XRD patterns of the samples when (t' +pyrochlore) mixtures with $z=0.5$ was used as the starting sample for the emf measurement.

(a): starting sample, (b): quenched at 1123 K.

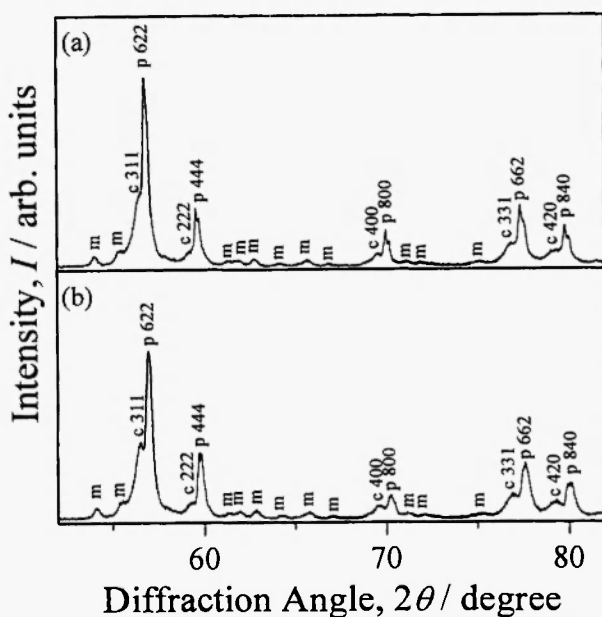


Fig. 7: XRD patterns of the samples when (t' +pyrochlore) mixtures with $z=0.5$ was used as the starting sample for the emf measurement.

(a): starting sample, (b): quenched at 923 K.

oxygen partial pressure, $p(\text{O}_2)$, over the sample powders decreased in this order. In Fig. 8, the $p(\text{O}_2)$ values at 973 K were plotted against the total composition, z in $\text{Ce}_2\text{Zr}_2\text{O}_{8-z}$, where the values for ($c+t$ +pyrochlore), (t' +pyrochlore) and ($c+m$ +pyrochlore) are indicated with Δ , \square and \circ , respectively. In the case of ($c+t$ +pyrochlore) and ($c+m$ +pyrochlore), the $p(\text{O}_2)$ appeared to be nearly constant independent of composition, z . The result indicates that the composition of $z=0.2\sim 0.5$ falls in the three phases region. In the case of (t' +pyrochlore), the $p(\text{O}_2)$ was changed with the value of z . Therefore, we can infer that the composition of $z=0.2\sim 0.5$ falls in the two phases region, and the tie line of t' -pyrochlore equilibrium does not lie on $(x_{\text{Ce}}/x_{\text{Zr}})=1$. The compositional dependences of $p(\text{O}_2)$ estimated roughly are shown with dashed lines in Fig. 8. Referring to Eq. [4], we can conclude that at 973 K,

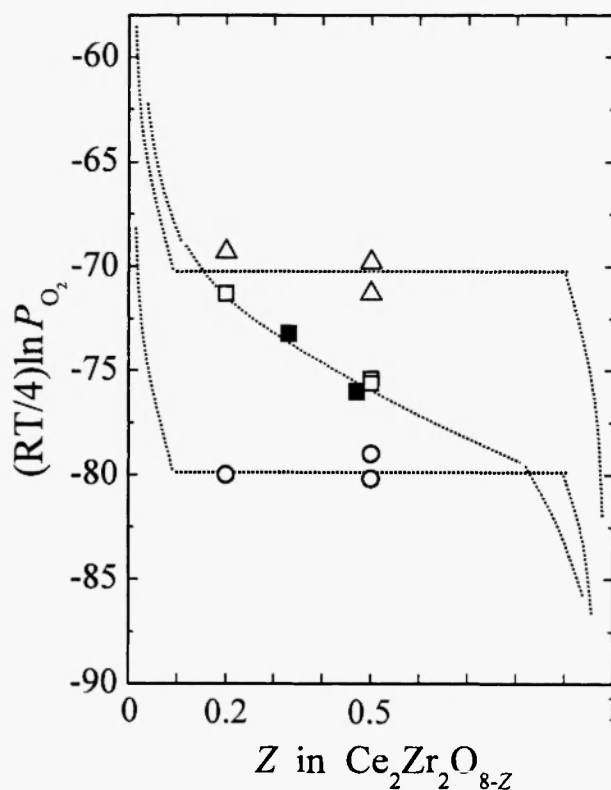


Fig. 8: Dependence of $p(\text{O}_2)$ over the mixed phases on composition z in $\text{Ce}_2\text{Zr}_2\text{O}_{8-z}$.

Δ : $c+t$ +pyrochlore (this work),

\square : t' +pyrochlore (this work),

\blacksquare : t' +pyrochlore /16/,

\circ : $c+m$ +pyrochlore (this work).

(c+m) mixture is thermodynamically the most stable, and t' phase is more stable than (c+t) mixture. According to the XRD analysis described above, at higher temperatures than 1373 K, the (c+t) mixture is thermodynamically the most stable. Thus, we reached the conclusion that the t' phase is metastable phase, however, its thermodynamic stability is very close to those of the most stable states; that is, (c+t) phases at high temperatures and (c+m) at low temperatures.

4. CONCLUSION

We have investigated the thermodynamic stability of metastable t'-Ce_{0.5}Zr_{0.5}O₂ phase, compared with those of ZrO₂-based monoclinic and tetragonal phases and CeO₂-based cubic phase. The various sample disks consisting of two or three phases mixture were annealed at higher temperatures than 1323 K, and then subjected to XRD analysis. In addition, the oxygen partial pressure over (t+pyrochlore), (c+t+pyrochlore), or (c+m+pyrochlore) powders was measured by use of the electrochemical cell involving a stabilized-zirconia solid electrolyte. The obtained results are as follows,

- (1) A single phase of t' decomposed into zirconia-based t phase and ceria-based c phase at higher temperatures than 1488 K. The t' phase containing a small amount of t and c decomposed at higher temperatures than 1373 K.
- (2) The result confirms that the t' phase is thermodynamically unstable; i.e., metastable. This is consistent with the phase diagram of CeO₂-ZrO₂ system reported. Because the precipitation of the t and c phases requires their nucleus, the single phase of t' is virtually stable at temperatures as high as 1473 K.
- (3) The oxygen partial pressure, $P(\text{O}_2)$, over the sample powders of (c+t+pyrochlore), (t'+pyrochlore) and (c+m+pyrochlore) decreased in this order. At lower temperatures than 1223 K, the thermodynamic stability increased in the order of (c+t), t', and (c+m).
- (4) The present experimental results have revealed that the t' phase is metastable; however, its thermodynamic stability is very close to those of (c+t) two phases at high temperatures and (c+m) at low temperatures.

REFERENCES

1. S. Matsumoto, *Toyota Tech. Rev.*, **44**, 12-17 (1994).
2. M. Ozawa, M. Kimura, and A. Isogai, *J. Alloys Compd.*, **193**, 73-75 (1993).
3. T. Murota, T. Hasegawa, S. Aozawa, H. Matsui, and M. Motoyama, *J. Alloys Compd.*, **193**, 298-299 (1993).
4. S. Otsuka-Yao, H. Morikawa, N. Izu, and K. Okuda, *J. Jpn. Inst. Met.*, **59**, 1237-1246 (1995).
5. B. Zhu, *Solid State Ion.*, **119**, 305-310 (1999).
6. K. Kawamura, K. Watanabe, Y. Nigara, A. Kaimai, T. Kawada, and J. Mizusaki, *J. Electrochem. Soc.*, **145**, 2552-2558 (1998).
7. E. Tani, M. Yoshimura, and S. Somiya, *J. Am. Ceram. Soc.*, **66**, 506-510 (1983).
8. M. Yashima, H. Takashina, M. Kakihana, and M. Yoshimura, *J. Am. Ceram. Soc.*, **77**, 1869-1874 (1994).
9. S. Meriani, *J. Physique*, **47**, C1-485-C1-489 (1986).
10. M. Yashima, K. Morimoto, N. Ishizawa, and M. Yoshimura, *J. Am. Ceram. Soc.*, **76**, 2865-2868 (1993).
11. T. Omata, H. Kishimoto, S. Otsuka-Yao-Matsuo, N. Ohtori, and N. Umesaki, *J. Solid State Chem.*, **147**, 573-583 (1999).
12. H. Kishimoto, T. Omata, S. Otsuka-Yao-Matsuo, K. Ueda, H. Hosono, and H. Kawazoe, *J. Alloys Compd.*, **312**, 94-103 (2000).
13. S. Otsuka-Yao-Matsuo, T. Omata, N. Izu, and H. Kishimoto, *J. Solid State Chem.*, **138**, 47-54 (1998).
14. N. Izu, H. Kishimoto, T. Omata, T. Yao, and S. Otsuka-Yao-Matsuo, *Sci. Tech. Adv. Mat.*, **2**, 443-448 (2001).
15. N. Izu, H. Kishimoto, T. Omata, and S. Otsuka-Yao-Matsuo, *J. Solid State Chem.*, **151**, 253-259 (2000).
16. S. Otsuka-Yao-Matsuo, N. Izu, T. Omata, and K. Ikeda, *J. Electrochem. Soc.*, **145**, 1406-1413 (1998).
17. K. Kiukkola and C. Wagner, *J. Electrochem. Soc.*, **104**, 379-387 (1957).
18. D. R. Gaskell, *Introduction to Metallurgical*

Thermodynamics, Scripta Pub. Co., Washington,
USA. 1973; p.317.